THE JOURNAL OF PHYSICAL CHEMISTRY C

Article

Cite This: J. Phys. Chem. C 2020, 124, 749−755

pubs.acs.org/JPCC

Adsorption-Induced Deformation of Microporous Solids: A New Insight from a Century-Old Theory

Alexander V. Neimark*,† and Ivan Grenev‡

†Department of Chemical and Biochemical Engineering, Rutgers University, 98 Brett Road, Piscataway, New Jersey 08854-8058, United States

‡Boreskov Institute of Catalysis, SB RAS, Novosibirsk 630090, Russia

Supporting Information

ABSTRACT: Potential adsorption theory (PAT) suggested by Polanyi back in 1914 is till date one of the most widely used practical methodologies for the treatment of gas adsorption on microporous materials. Here, we extend PAT to the description of the phenomenon of adsorption-induced deformation, which has been recently attracting widespread interest of various scientific communities, from adsorption separations and energy storage to hydrocarbon recovery and carbon dioxide sequestration to drug delivery and actuators. A universal relationship is established between the stress caused by the interactions of guest molecules with the pore walls and the adsorption isotherm. It is shown that in the course of adsorption, microporous solids exhibit a non-monotonic deformation, with contraction at low gas pressures and expansion as the pressure increases. The proposed theory is verified with the experimental data on benzene and *n*-hexane adsorption on AR-V microporous carbon over a wide range of temperatures. It allows for predicting the adsorption deformation at different temperatures and with different adsorbates and can be applied to a wide class of microporous solids.

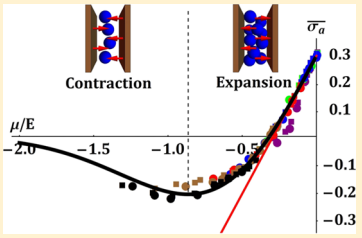

I. INTRODUCTION

Phenomenon of the deformation of nanoporous materials in the process of gas adsorption has been recently attracting considerable interest of various scientific communities, from adsorption separations and energy storage in metal−organic frameworks (MOFs) to hydrocarbon recovery in shales and carbon dioxide sequestration in coal to drug delivery and actuators.[1−12] While most materials expand or swell upon uptake of host species, microporous solids, with pores smaller than 2 nm, exhibit a counterintuitive behavior: upon adsorption with increase in gas pressure, the sample first contacts and then expands. Such a non-monotonic deformation is characteristic to all microporous materials, such as active carbons, zeolites, clays, and MOFs.[13−16] Although the experimental observation of this phenomenon is well-documented in the literature, a quantitative theory capable of predicting the deformation of adsorbents based on the information about adsorption properties of the materials is lacking. Here, we present a robust thermodynamic theory that links the adsorbent strain with the independently measured adsorption isotherm and allows for predicting the adsorption deformation at different temperatures and with different adsorbates. The proposed approach is based on the classical potential adsorption theory (PAT) suggested by Polanyi[17,18] back in 1914 and later elaborated by Dubinin and co-workers[19−21] into the most widely used practical methodology of characterization of microporous solids, known as the theory of volume filling of micropores (TVFM).

II. THERMODYNAMICS OF ADSORPTION-INDUCED DEFORMATION IN TERMS OF POTENTIAL ADSORPTION THEORY

In addition to the external pressure P_{ext}, deformation of a porous solid is caused by the adsorption stress σ_a, exerted by the guest molecules interacting with the pore walls.[22] The volumetric strain ϵ of an isotropic sample in the elastic linear approximation is defined by the volumetric modulus K

$$\epsilon = (\sigma_a - P_{ext})/K = P_{sol}/K \quad (1)$$

In gas adsorption experiments with free standing samples, the external pressure, P_{ext}, equals the bulk gas pressure, and the difference between the adsorption stress and the bulk gas pressure is commonly called the solvation pressure, $P_{sol} = \sigma_a - P$.[23,24] From the thermodynamic standpoint,[22,25] the adsorption stress σ_a is rigorously defined as the derivative of the grand thermodynamic potential of the adsorbed phase $\Omega_a(\mu, V, T)$ with respect to the variation of the sample volume, or the pore volume V, provided the solid phase is incompressible, at the given chemical potential μ of the adsorbate and temperature T

$$\sigma_a(\mu, T) = (-\partial\Omega_a(\mu, V, T)/\partial V)_{\mu,T} \quad (2)$$

The grand thermodynamic potential of the adsorbed phase Ω_a, which is commonly referred to in the adsorption literature as

Received: October 25, 2019
Revised: December 4, 2019
Published: December 5, 2019

DOI: 10.1021/acs.jpcc.9b10053
J. Phys. Chem. C 2020, 124, 749−755

the integral work of adsorption, is related to the adsorption isotherm, $a(\mu, V, T)$, via the Gibbs equation

$$\Omega_a(\mu, V, T) = -\int_{-\infty}^{\mu} a(\mu, V, T)\mathrm{d}\mu \tag{3}$$

The chemical potential is commonly reckoned from the saturation state

$$\mu = -RT\ \ln[f_0/f] \approx -RT\ \ln[P_0/P] \tag{4}$$

where f is fugacity; the second equality implies the ideal gas approximation. As such, to predict the adsorption deformation through eqs 1−3, it is necessary to know the theoretical equation for the adsorption isotherm $a(\mu, V, T)$.

According to PAT, the adsorption isotherm of a vapor at given pressure P and temperature T is presented as a universal function of the adsorbate chemical potential μ reduced by a characteristic energy of adsorption E

$$a(P, T) = a_0(V, T)f(-\mu/E) \tag{5}$$

Function $f(-\mu/E)$, called the characteristic curve, is related to the integral volume distribution of the adsorption potential inside the micropores and is normalized ($f(0) = 1$). $f(-\mu/E)$, which is supposed to be independent of temperature and adsorbate, represents the degree of pore filling, $\theta = a/a_0 = f(-\mu/E)$. Here, a_0 is the adsorption capacity at the saturation pressure P_0, which depends on temperature T and is represented through the pore volume V and the molar volume v_l of liquid adsorbate

$$a_0(V, T) = V/v_l(T) \tag{6}$$

Equation 5 represents the Gurvich rule that serves as a practical definition of the pore volume. The characteristic adsorption energy E depends on the adsorbate. Choosing the adsorption energy of one particular adsorbate (traditionally, benzene) E_0 as a reference, E for another adsorbate is presented using the affinity coefficient β as $E = \beta E_0$.[19,20] Once the characteristic curve function f is determined by fitting the experimental isotherm for one adsorbate at a particular temperature, the adsorption isotherms at other temperatures and for other adsorbates can be predicted.

TVFM models employ particular equations of the characteristic curve. The most popular is the Dubinin−Radushkevich (DR) equation[26]

$$\theta = a(\mu, V, T)/a_0(V, T) = f(-\mu/E) = \exp[-(\mu/\beta E_0)^2] \tag{7}$$

which has only one parameter, characteristic adsorption energy E_0. PAT and TVFM have important predictive capabilities. In the works of Dubinin and his co-workers and followers, one can find numerous examples of successful applications of TVFM for a wide range of adsorbates and various microporous adsorbents, mainly carbons and zeolites.[13,16,21,27,28] In this work, we demonstrate that PAT and, in particular, the DR equation provide a practical approach to predict the deformation of microporous carbons in the course of adsorption.

Using the characteristic curve function $f(-\mu/E)$, the grand thermodynamic potential Ω_a, is presented

$$\Omega_a(\mu, V, T) = -a_0(V, T)\int_{-\infty}^{\mu} f(-\mu/E)\mathrm{d}\mu$$
$$= -a_0 E\int_{-\mu/E}^{\infty} f(x)\mathrm{d}x \tag{8}$$

Accounting for the expression 8, the adsorption stress in PAT is presented in a compact form

$$\sigma_a(\mu, T) = -\frac{\mathrm{d}\ln a_0}{\mathrm{d}V}\Omega_a(\mu, V, T) - \frac{\mathrm{d}\ln E}{\mathrm{d}V}\int_0^a \mu\ \mathrm{d}a \tag{9}$$

It is worth noting that the strain and stress in eq 1, the grand thermodynamic potential Ω in eqs 3 and 8, and stress in eq 9 are reckoned from the hypothetical "dry" vacuumed state of $P = 0$ and $\mu = -\infty$. This must be taken into account while analyzing the experimental data, which is reckoned from a certain experimentally measured reference state.

III. GENERAL FEATURES OF ADSORPTION-INDUCED DEFORMATION IN MICROPOROUS SOLIDS

Equation 9 allows to evaluate general qualitative trends of the adsorption stress. Note that the derivative of the total adsorption capacity with respect to the sample pore volume, $\mathrm{d}\ln a_0/\mathrm{d}V$, is always positive, as larger pores have more space to host molecules. According to the Gurvich rule (2), $\mathrm{d}\ln a_0/\mathrm{d}V \approx 1/V_0 > 0$, where V_0 is the sample reference volume in the dry state. At the same time, the derivative of the adsorption energy is always negative, $\mathrm{d}\ln E/\mathrm{d}V = -\lambda/V_0 < 0$; adsorption energy in smaller pores is higher; λ is the energy susceptibility factor. As such, the first term in the LHS of eq 9 is positive ($\Omega_a < 0$), while the second term is negative ($\int_0^a \mu\ \mathrm{d}a < 0$). The fact that the effects of the capacity and energy variations with deformation have opposite signs explains the observed non-monotonic strain in the course of gas adsorption on microporous adsorbents. At low gas pressures and loose pore loading, the energy variation effect dominates, causing pore contraction: due to attractive adsorption interactions, guest molecules serve as couplings between opposite pore walls. At sufficiently high gas pressures, the volume variation effect dominates, causing pore expansion: the pores become crowded with guest molecules, which repel and "elbow" each other, exerting a positive stress on the pore walls.

Typical theoretical dependencies of the adsorption and stress isotherms are presented in Figure 1 as functions of μ/E, drawing on an example of the DR equation. The stress is non-monotonic: it decreases in the beginning of adsorption at low pressure, achieves a minimum, and then increases to approach a linear asymptote at a sufficiently high pressure. Correspondingly, the sample deformation is expected to be non-monotonic with contraction as the stress decreases and with expansion as the stress increases.

The adsorption stress in the beginning of adsorption at low gas pressures, when $-\mu \gg E$ and $-\mu a \gg -\Omega_a$, has the following general asymptote

$$\sigma_a(\mu, T) \approx -\frac{\mathrm{d}\ln E}{V}\mu a(\mu, V, T)$$
$$= -\frac{\mathrm{d}\ln E}{\mathrm{d}V}\mu\ a_0(V, T)f\left(-\frac{\mu}{E}\right) \tag{10}$$

As the chemical potential increases, the adsorption stress, which originates from zero at $\mu = -\infty$, is negative and progressively decreases, causing the sample to contract. This

DOI: 10.1021/acs.jpcc.9b10053
J. Phys. Chem. C 2020, 124, 749−755

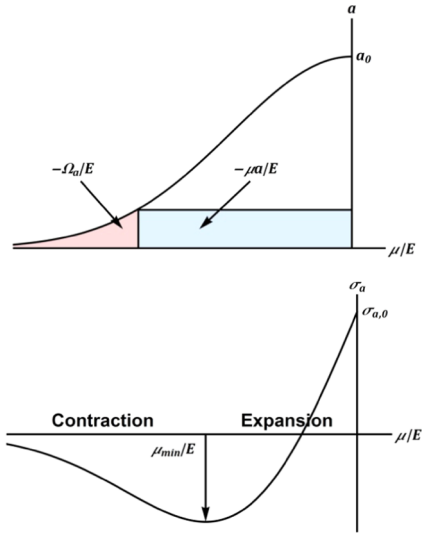

Figure 1. Typical theoretical dependencies of the adsorption and stress isotherms as functions of the reduced adsorbate chemical potential, μ/E.

behavior is typical for any microporous solid, provided the sample is evacuated at sufficiently low pressures.[13]

The adsorption stress at conditions of complete pore filling at sufficiently high pressures, when $-\mu \ll E$, $a(\mu, V, T) \approx a_0$, and $\Omega_a = \Omega_a|_{\mu=0} + \int_\mu^0 a(\mu, V, T)d\mu \approx \Omega_{a,0} - \mu a_0$ ($\Omega_{a,0} = \Omega_a|_{\mu=0}$), follows the universal behavior

$$\sigma_a(\mu, T) \approx \sigma_{a,0} + \mu/v_l = \sigma_{a,0} + P_{cap} - (P_0 - P) \quad (11)$$

Here, $\sigma_{a,0} = \sigma_a|_{\mu=0}$ is the adsorption stress at the fully saturated conditions, $P = P_0$ and $\mu = 0$ and P_{cap} is the capillary, or Laplace, pressure of the liquid adsorbate having the same chemical potential as the adsorbed phase. According to the Hückel equation[29]

$$P_{cap} = \mu/v_l + (P_0 - P) = -(RT/v_l)\ln[f_0/f] + (P_0 - P)$$
$$\approx -(RT/v_l)\ln[P_0/P] \quad (12)$$

The latter equality represents the Kelvin–Laplace equation and is valid for the ideal gas approximation that is standard for adsorption experiments well below the critical temperature, when $-\mu/v_l \gg (P_0 - P)$. Equations 11 and 12 imply that the adsorption stress and the induced strain, respectively, are linear functions of the capillary pressure P_{cap} or the logarithm of relative pressure, $\ln[P_0/P]$. It is instructive to present this linear dependence using the strain, $\epsilon_0 = \epsilon - \epsilon|_{\mu=0}$, reckoned from the sample strain at a fully saturated state at $P = P_0$ and $\mu = 0$, $P_{cap} = 0$. With these assumptions, eq 1 is transformed into

$$\epsilon_0 = \epsilon - \epsilon|_{\mu=0} = P_{cap}/K \approx -(RT/v_l)\ln[P_0/P]/K \quad (13)$$

The linear relationship (eq 13) holds as the asymptote of the general eq 1 at sufficiently high pressures. This conclusion has very important implications for the correlation of the theoretical predictions and experimental data. Indeed, the experimental strain isotherms typically exhibit a linear behavior in the region of complete pore filling. It is noteworthy that the linear relationship (eq 1), known as the capillary approximation,[14] is a characteristic not only of microporous but also of mesoporous materials filled by capillary condensed fluid.[30−32] Theoretically, it was established by Gor and Neimark[14] for mesoporous adsorbents using the Derjaguin–Broekhoff–de Boor (DBDB) model of capillary condensation. Equation 13 can be used to determine the effective volumetric modulus K from the slope of the experimental strain isotherm plotted in semi-logarithmic coordinates.[30] This modulus is sometimes called the pore load modulus.[31]

Of special interest is the condition of the minimum of strain isotherm, which corresponds to the maximum contraction. This condition reflects the so called "most convenient" packing of guest molecules when the coupling and crowding effects compensate each other.[22] The point of maximum contraction is determined from the condition of the maximum pore filling with respect to the pore size at a given chemical potential

$$\left.\frac{\partial\sigma_a}{\partial\mu}\right|_{V,T} = -\frac{\partial^2\Omega_a}{\partial\mu\partial V} = -\frac{\partial^2\Omega_a}{\partial V\partial\mu} = \left.\frac{\partial a}{\partial V}\right|_{\mu,T} = 0 \quad (14)$$

It is instructive to present the equations of PAT in the dimensionless form, expressing the adsorbed amount as the degree of pore filling, $\theta = a/a_0 = f(-\mu/E)$, and reducing the adsorption stress by its characteristic value $\sigma_a^* = Ea_0/V_0 \approx E/v_l$. Using the dimensionless adsorption stress, $\overline{\sigma_a} = \sigma_a/[Ea_0/V_0]$, eq 8 transforms into a general form

$$\overline{\sigma_a}(\mu/E) = \int_{-\mu/E}^{\infty} f(x)dx + \lambda\int_0^{\theta}(\mu/E)d\theta$$
$$= (1-\lambda)\int_{-\mu/E}^{\infty} f(x)dx + \lambda(\mu/E)f(-\mu/E) \quad (15)$$

Here, the energy susceptibility factor $\lambda = -(d\ln E/dV)/V_0$ is the only dimensionless parameter that should be determined from the experimental data. Note that the stress at the saturation, $\sigma_{a,0}$ is

$$\overline{\sigma_{a,0}} = \int_0^{\infty} f(x)dx + \lambda\int_0^1(\mu/E)d\theta = (1-\lambda)\int_0^{\infty} f(x)dx \quad (16)$$

The characteristic value of adsorption stress, $\sigma_a^* = Ea_0/V_0$, is on the order of 1000 atm, which may result in strain within ~0.1–1%. For the example of benzene adsorption on AR-V microporous carbon considered below,[33] $\lambda = 0.67$, $\overline{\sigma_{a,0}} = \frac{\sqrt{\pi}}{2}(1-\lambda) = 0.292$ and $\sigma_a^* = 0.17$ GPa.

IV. CORRELATION OF THEORY AND EXPERIMENTS

There are several important aspects that should be taken into account while correlating the theoretical relationships for the adsorption stress derived above with the experimental strain isotherms. The strain isotherms on microporous adsorbents are usually measured by dilatometry using the specially prepared samples in the form of cylindrical rods. These experiments treat free standing samples, so that the measured linear strain is one third of the volumetric strain.

For small elastic deformations, it is reasonable to assume that the sample compressibility does not depend on adsorption and the volumetric modulus K determined from the slope of the linear region of the strain isotherm according to eq 13 can be used in the general eq 1 in the whole range of pressures to relate the strain and stress isotherms. As such, the theoretical prediction can be made for the strain, $\epsilon_0 = \epsilon - \epsilon|_{\mu=0}$, reckoned from the sample strain at a fully saturated state, rewriting eq 1 as

$$\epsilon_0 = [(\sigma_a - P) - (\sigma_{a,0} - P_0)]/K \approx (\sigma_a - \sigma_{a,0})/K \quad (17)$$

DOI: 10.1021/acs.jpcc.9b10053
J. Phys. Chem. C 2020, 124, 749−755

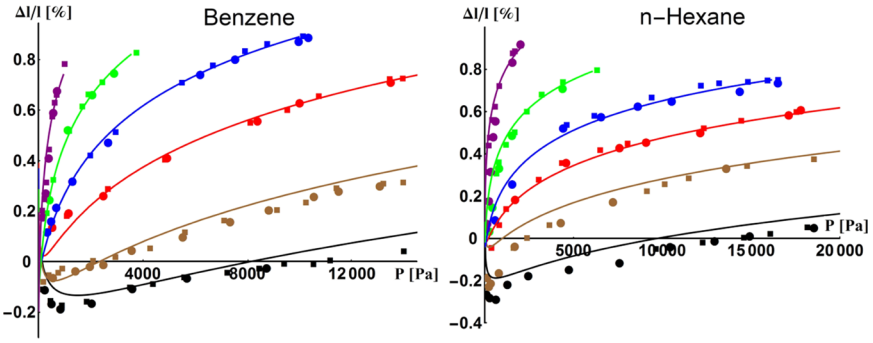

Figure 2. Strain isotherms of benzene and *n*-hexane at 353 K (black), 333 K (brown), 313 K (red), 293 K (blue), 273 K (green), and 255 K (purple). Circles, adsorption; squares, desorption. Lines correspond to the theoretical predictions by eq 25 with $\lambda = 0.67$, $K = 3$ GPa, and offset strains $\Delta l_0/l$ given in Table S1.

The latter approximate equality is valid, provided that the adsorption stress is significantly larger than the gas pressure, $|\sigma_a| \gg P$, and the sample deformation caused by the external pressure is neglected. We will use this approximation in further discussion.

It is noteworthy that experimental measurements do not start from an ideal dry state but rather from the lowest available pressure, $P = P_1$. The first point measured by dilatometry at the lowest pressure P_1 is usually taken as a reference for an experimentally defined strain: $\epsilon_{exp}(P_1) = 0$. This initial state is prestressed compared to a fully saturated state. The prestress $\Delta\sigma_{a,1} = \sigma_{a,1} - \sigma_{a,0}$ ($\sigma_{a,1} = \sigma_a(\mu_1, T)$) reflects the shrinkage of the samples upon desorption from the fully saturated state to the initial state

$$\Delta\sigma_{a,1} = \sigma_a^*\left[-(1-\lambda)\int_0^{-\mu_1/E} f(x)\mathrm{d}x + \lambda(\mu_1/E)f(-\mu_1/E)\right] \tag{18}$$

As such, the experimentally measured strain ϵ_{exp} is correlated with the stress reckoned from the prestress $\sigma_{a,1}$

$$\begin{aligned}\epsilon_{exp} &= (\sigma_a(\mu, T) - \sigma_{a,1})/K = \left\{\frac{\mathrm{dln}\, a_0}{\mathrm{d}V}[\Omega_a(\mu, V, T) - \Omega_a(\mu_1, V, T)] - \frac{\mathrm{dln}\, E}{\mathrm{d}V}\int_{a_1}^{a}\mu\,\mathrm{d}a\right\}/K \\ &= [\sigma_a^*/K]\left[(1-\lambda)\int_{-\mu/E}^{-\mu_1/E} f(x)\mathrm{d}x - \lambda(\mu/E)f(-\mu/E) + \lambda(-\mu_1/E)f(-\mu_1/E)\right]\end{aligned} \tag{19}$$

It is noteworthy that eq 19 can be used with any type of isotherm, $a(\mu)$, that obeys the PAT assumptions. One option is to use a properly smoothened interpolated experimental isotherm.

Equation 19 has two parameters, K and λ, which are defined from the correlation with the experimental strain isotherm. The bulk modulus K can be unambiguously determined from the strain isotherm slop in the linear region of high loadings (eq 13). The energy susceptibility factor λ can be chosen to match the position, $\mu = \mu_{min}$, of the maximum contraction, which is determined by eq 14, or, equivalently, directly from eq 19 by equating to zero the derivative

$$\left.\frac{\mathrm{d}\epsilon_{exp}}{\mathrm{d}\mu}\right|_{\mu=\mu_{min}} = 0 \tag{20}$$

For the DR type of isotherm, eqs 14 and eq19 imply

$$\lambda = \frac{1}{2}\left(\frac{E}{\mu_{min}}\right)^2 \tag{21}$$

Let us demonstrate the applicability of the proposed model for the case of the DR eq 7. According to eq 3, the grand thermodynamic potential Ω_a can be expressed, as

$$\Omega_a(\mu, V, T) = -\frac{\sqrt{\pi}}{2}a_0\beta E_0(1 - \mathrm{Erf}[-\mu/\beta E_0]) \tag{22}$$

Correspondinly, the adsorption stress, eq 2, is presented, as

$$\sigma_a(\mu, T) = \sigma_a^*\left\{-\lambda(-\mu/\beta E_0)\exp[-(\mu/\beta E_0)^2] + \frac{\sqrt{\pi}}{2}(1-\lambda)(1 - \mathrm{Erf}[-\mu/\beta E_0])\right\} \tag{23}$$

and the experimental volumetric strain, eq 19, is converted into the following form

$$\epsilon_{exp} = \left\{-\lambda[(-\mu/\beta E_0)\exp[-(\mu/\beta E_0)^2] - (-\mu_1/\beta E_0)\exp[-(\mu_1/\beta E_0)^2]] + \frac{\sqrt{\pi}}{2}(1-\lambda)(\mathrm{Erf}[-\mu/\beta E_0] - \mathrm{Erf}[-\mu_1/\beta E_0])\right\}\sigma_a^*\Big/K \tag{24}$$

The characteristic magnitude of the adsorption stress, $\sigma_a^* = E/v_l$, is proportional to the adsorption energy. The relative linear adsorption-induced strain, $\Delta l/l$, is expressed as

$$\frac{\Delta l}{l} = \left\{-\lambda(-\mu/\beta E_0)\exp[-(\mu/\beta E_0)^2] + \frac{\sqrt{\pi}}{2}(1-\lambda)(1 - \mathrm{Erf}[-\mu/\beta E_0])\right\}\sigma_a^*/3K + \frac{\Delta l_0}{l} \tag{25}$$

Here, $\Delta l_0/l$ is the offset strain constant equal to the experimentally measured (or extrapolated) linear strain at the approach of saturation, at $P/P_0 \to 1$. In the region of linear deformation, the capillary approximation (eq 12) holds, and

$$\Delta l/l \approx \frac{-(RT/v_l)\ln[P_0/P]}{3K} + \Delta l_0/l \tag{26}$$

DOI: 10.1021/acs.jpcc.9b10053
J. Phys. Chem. C 2020, 124, 749−755

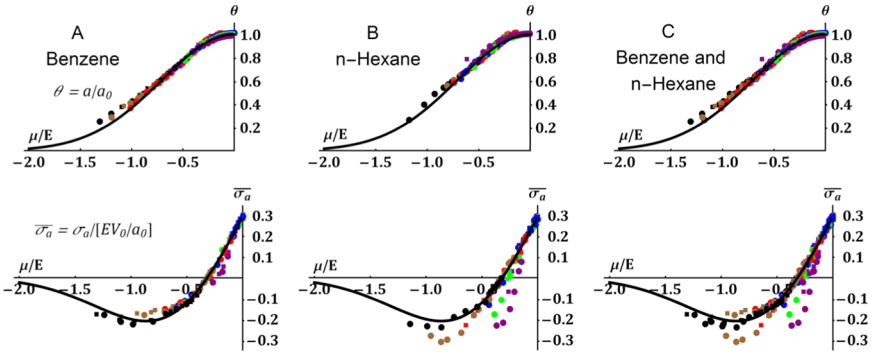

Figure 3. Universal dimensionless isotherms of the degree of filling, $\theta = a/a_0$, (upper raw) and the reduced adsorption stress, $\overline{\sigma_a} = \sigma_a/[EV_0/a_0]$, (lower raw) as functions of the reduced adsorbate chemical potential, μ/E. Lines correspond to the DR characteristic curve (eq 7), and the correspondingly reduced stress (eq 15). Experimental data on AR-V carbon for (A) benzene[33] and (B) *n*-hexane[34] at 353 K (black), 333 K (brown), 313 K (red), 293 K (blue), 273 K (green), and 255 K (purple). The circle symbols correspond to adsorption and square symbols to the desorption data. (C) Combined benzene and *n*-hexane data.

The linear correlation (eq 26) makes it possible to determine the volumetric modulus K and the offset strain $\Delta l_0/l$ from the slope and onset of the experimental strain isotherm plotted in semi-log coordinates, as shown in Figures S1 and S2 presented in the Supporting Information. Additional discussion on the offset strain determination is given in the Supporting Information.

The predictive capabilities of the proposed method are demonstrated based on the experimental data of the adsorption of benzene[33] and *n*-hexane[34] on the AR-V carbon microporous adsorbent in the range of temperatures from 255 to 353 K. AR-V carbon is produced from coal dust and adhesion agents by steam treatment at 1100 K−1200 K. The experimental adsorption isotherms of benzene and *n*-hexane at different temperatures in the linear form of the DR equation ($\log[V_0]$ as functions of μ^2/β^2 (see Figure S3)) collapse into one characteristic curve with the pore volume $V_0 = 0.26$ cm^3/g and characteristic energy $E_0 = 14.3$ kJ/mol for benzene obtained from the fitting of experimental adsorption isotherms; the affinity coefficient $\beta = 1.29$ for *n*-hexane is taken from ref 35.

Figure 2 show the theoretical strain isotherms calculated according to eq 25 in comparison with the experimental deformation. The factor $\lambda = 0.67$ was determined from the strain isotherms of benzene at 353 and 333 K according to eq 21, since the position of the strain minimum is clearly defined on these isotherms. The effective bulk modulus $K = 3$ GPa was determined according to eq 26 from the slope of linear regions of the strain isotherms of benzene in semi-logarithmic coordinates at 273 and 293 K, since the measurements at these temperatures were performed up to the saturation pressure. The offset strains $\Delta l_0/l$, which varied from 0.5 to 0.9%, were determined with $K = 3$ GPa according to eq 26 from linear regions of strain isotherms or from fitting to eq 25 in case of high temperatures 333 and 353 K, when data at high pressures were not available. The experimental strain isotherms in semi-logarithmic coordinates for different temperatures and the linear capillary approximation plots are presented in Figures S1 and S2, respectively. All parameters used in the calculations are presented in Table S1.

In both cases of benzene and *n*-hexane adsorption, only two experimental strain isotherms at 353 and 333 K possess a contraction region. The strain, experimentally measured at lower temperatures from 255 to 313 K, is positive and increases monotonically. This is explained by the fact that the contraction region was outside the range of measured pressures. Indeed, the pressure P_{min}, which corresponds to the maximum contraction, progressively decreases with decreasing temperature (see Table S2). According to eq 21, P_{min} is estimated for benzene as 1500, 600, and 210 Pa at 353, 333, and 313 K, respectively. While the P_{min} values at 353 and 333 K reasonably fit the strain minimum, the value of 210 Pa is outside the range of the measured pressures at 313 K. The proposed theoretical relationship fits well the strain isotherms in the expansion region of relatively high pressures, which confirms the validity of the linear capillary approximation (eq 26) employed for the determination of the volumetric modulus K and the offset strain $\Delta l_0/l$. The *n*-hexane strain isotherms exhibit similar behaviors as those of benzene, although the fit to the theoretical relationship at low pressures is apparently worse. However, the fact that the affinity coefficient for *n*-hexane was taken from the literature and the fitting was done only for the reference adsorption energy of benzene confirms the predictive capabilities of the proposed theory.

Figure 3 presents the universal dimensionless theoretical dependencies of the degree of filling, $\theta = a/a_0$, for the DR eq 7 and the correspondingly reduced adsorption stress, $\overline{\sigma_a} = \sigma_a/[E/v_l]$, eq 15, as functions of the reduced adsorbate chemical potential, μ/E, in comparison with the experimental data on benzene[33] and *n*-hexane[34] on AR-V carbon. $\overline{\sigma_a}$ calculated with the parameters, $E_0 = 14.3$ kJ/mol and $\lambda = 0.67$, established from the benzene data. The experimental stress data are recalculated from the strain data from Figure 2 with the volumetric modulus, $K = 3$ GPa. Agreement between the theoretical predictions and experimental data is excellent, accounting for the known deficiency of the DR equation at low loadings and the natural spread of the experimental data.

V. CONCLUSIONS

The universal relationships are established for predicting the deformation of microporous solids induced by the adsorption of different adsorbates in a wide range of temperatures. The proposed model is based on only three parameters, adsorption energy E, energy susceptibility factor λ, and volumetric modulus K, which can be determined from the experimental data for a reference adsorbate at a particular temperature. The main quantitative marker of the effect of adsorption deformation is the characteristic adsorption stress, $\sigma_a^* = E/v_l$.

DOI: 10.1021/acs.jpcc.9b10053
J. Phys. Chem. C 2020, 124, 749−755

The smaller the pore, the larger the adsorption energy and the corresponding adsorption stress. It is noteworthy that the proposed relationship for the adsorption stress contains only one parameter, the energy susceptibility factor λ, which cannot be defined independently from the experimental adsorption isotherm; this parameter was determined from the pressure of maximum contraction on the benzene strain isotherm. The non-monotonic behavior of the strain isotherm is defined by λ. Conversion of the experimental strain into stress requires the effective bulk modulus K and the offset strain $\Delta l_0/l$ that are obtained straight from the linear asymptotic region of the strain isotherms in semi-logarithmic coordinates at high pressures. The offset strain $\Delta l_0/l$ depends on the lowest measured pressure and may vary from one experiment to another. While for rigid microporous solids like carbons the adsorption strain is typically small, the adsorption stress on the order of thousands of atmospheres can compromise the material integrity, which is specifically important in the case of geosorbents like coal. In softer materials, such as metal–organic frameworks, the adsorption stress may induce a larger deformation causing phase transformations in the frameworks, known as breathing and gate-opening.[3,36−38] In this case, the proposed model could be applied for analysis of elastic deformation that precedes the phase transformation, which is associated with plastic deformation occurring upon achieving a threshold adsorption stress according to the ansatz suggested in ref 39. The general eqs 15 and 19 for the adsorption stress and strain, respectively, can be used with more complex adsorption models than the DR equation model and extended to other classes of materials, provided the assumptions of the PAT are met, deformation proceeds in a linear elastic regime, and the effects of material anisotropy can be neglected.

■ ASSOCIATED CONTENT

Supporting Information

The Supporting Information is available free of charge at https://pubs.acs.org/doi/10.1021/acs.jpcc.9b10053.

Experimental strain isotherms of benzene and *n*-hexane adsorption at 273−333 K fitted with the linear asymptote of capillary approximation (Figures S1 and S2); experimental isotherms of benzene and *n*-hexane adsorption at 313−353 K in the coordinates of the DR equation (Figure S3); parameters used in the calculations of strain isotherms (Table S1); condition of maximum contraction and corresponding pressure P_{min} (Table S2); and determination of the offset strain (Table S3) (PDF)

■ AUTHOR INFORMATION

Corresponding Author

*E-mail: aneimark@rutgers.edu.

ORCID

Alexander V. Neimark: 0000-0002-3443-0389

Notes

The authors declare no competing financial interest.

■ ACKNOWLEDGMENTS

The work was supported by the National Science Foundation (grant no. 1834339) and the Ministry of Science and Higher Education of the Russian Federation (Project AAAA-A17-117041710079-8).

■ REFERENCES

(1) Vandamme, M. Coupling between adsorption and mechanics (and vice versa). *Curr. Opin. Chem. Eng.* **2019**, *24*, 12−18.

(2) Agrawal, M.; Bhattacharyya, S.; Huang, Y.; Jayachandrababu, K. C.; Murdock, C. R.; Bentley, J. A.; Rivas-Cardona, A.; Mertens, M. M.; Walton, K. S.; Sholl, D. S.; Nair, S. Liquid-Phase Multicomponent Adsorption and Separation of Xylene Mixtures by Flexible MIL-53 Adsorbents. *J. Phys. Chem. C* **2018**, *122*, 386−397.

(3) Aljammal, N.; Jabbour, C.; Chaemchuen, S.; Juzsakova, T.; Verpoort, F. Flexibility in Metal-Organic Frameworks: A Basic Understanding. *Catalysts* **2019**, *9*, No. 512.

(4) Perrier, L.; Pijaudier-Cabot, G.; Gregoire, D. Extended poromechanics for adsorption-induced swelling prediction in double porosity media: Modeling and experimental validation on activated carbon. *Int. J. Solids Struct.* **2018**, *146*, 192−202.

(5) Ho, T. A.; Wang, Y. F.; Criscenti, L. J. Chemo-mechanical coupling in kerogen gas adsorption/desorption. *Phys. Chem. Chem. Phys.* **2018**, *20*, 12390−12395.

(6) Allen, A. J.; Espinal, L.; Wong-Ng, W.; Queen, W. L.; Brown, C. M.; Kline, S. R.; Kauffman, K. L.; Culp, J. T.; Matranga, C. Flexible metal-organic framework compounds: In situ studies for selective CO2 capture. *J. Alloys Compd.* **2015**, *647*, 24−34.

(7) Espinoza, D. N.; Vandamme, M.; Dangla, P.; Pereira, J. M.; Vidal-Gilbert, S. Adsorptive-mechanical properties of reconstituted granular coal: Experimental characterization and poromechanical modeling. *Int. J. Coal Geol.* **2016**, *162*, 158−168.

(8) Horcajada, P.; Serre, C.; Maurin, G.; Ramsahye, N. A.; Balas, F.; Vallet-Regi, M.; Sebban, M.; Taulelle, F.; Ferey, G. Flexible porous metal-organic frameworks for a controlled drug delivery. *J. Am. Chem. Soc.* **2008**, *130*, 6774−6780.

(9) Ganser, C.; Fritz-Popovski, G.; Morak, R.; Sharifi, P.; Marmiroli, B.; Sartori, B.; Amenitsch, H.; Griesser, T.; Teichert, C.; Paris, O. Cantilever bending based on humidity-actuated mesoporous silica/silicon bilayers. *Beilstein J. Nanotechnol.* **2016**, *7*, 637−644.

(10) Tanaka, H.; Miyahara, M. T. Free energy calculations for adsorption-induced deformation of flexible metal-organic frameworks. *Curr. Opin. Chem. Eng.* **2019**, *24*, 19−25.

(11) Evans, J. D.; Krause, S.; Kaskel, S.; Sweatman, M. B.; Sarkisov, L. Exploring the thermodynamic criteria for responsive adsorption processes. *Chem. Sci.* **2019**, *10*, 5011−5017.

(12) Vanduyfhuys, L.; Rogge, S. M. J.; Wieme, J.; Vandenbrande, S.; Maurin, G.; Waroquier, M.; Van Speybroeck, V. Thermodynamic insight into stimuli-responsive behaviour of soft porous crystals. *Nat. Commun.* **2018**, *9*, No. 204.

(13) Tvardovskiy, A. V. *Sorbent Deformation*, 1st ed.; Elsevier Academic Press:Amsterdam, Boston, 2007; p 278.

(14) Gor, G. Y.; Neimark, A. V. Adsorption-Induced Deformation of Mesoporous Solids. *Langmuir* **2010**, *26*, 13021−13027.

(15) Balzer, C.; Brameier, S.; Neimark, A. V.; Reichenauer, G. Deformation of Microporous Carbon during Adsorption of Nitrogen, Argon, Carbon Dioxide, and Water Studied by in Situ Dilatometry. *Langmuir* **2015**, *31*, 12512−12519.

(16) Fomkin, A. A.; Shkolin, A. V.; Pulin, A. L.; Men'shchikov, I. E.; Khozina, E. V. Adsorption-Induced Deformation of Adsorbents. *Colloid J.* **2018**, *80*, 578−586.

(17) Polanyi, M. Adsorption from the point of view of the of the Third Law of Thermodynamics. *Verh. Deut. Phys. Ges.* **1914**, *16*, 1012−1016.

(18) Polanyi, M. The Potential Theory of Adsorption. *Science* **1963**, *141*, 1010−1013.

(19) Dubinin, M. M. The Potential Theory of Adsorption of Gases and Vapors for Adsorbents with Energetically Nonuniform Surfaces. *Chem. Rev.* **1960**, *60*, 235−241.

(20) Dubinin, M. M. Fundamentals of the theory of adsorption in micropores of carbon adsorbents: Characteristics of their adsorption properties and microporous structures. *Carbon* **1989**, *27*, 457−467.

(21) Dubinin, M. M.; Polyakov, N. S.; Kataeva, L. I. Basic properties of equations for physical vapor adsorption in micropores of carbon

DOI: 10.1021/acs.jpcc.9b10053
J. Phys. Chem. C 2020, 124, 749−755

adsorbents assuming a normal micropore distribution. *Carbon* **1991**, *29*, 481−488.
(22) Ravikovitch, P. I.; Neimark, A. V. Density functional theory model of adsorption deformation. *Langmuir* **2006**, *22*, 10864−10868.
(23) Evans, R.; Marconi, U. M. B. Phase-Equilibria and Solvation Forces for Fluids Confined between Parallel Walls. *J. Chem. Phys.* **1987**, *86*, 7138−7148.
(24) Balbuena, P. B.; Berry, D.; Gubbins, K. E. Solvation Pressures for Simple Fluids in Micropores. *J. Phys. Chem. A* **1993**, *97*, 937−943.
(25) Neimark, A. V. In *Reconciliation of Gibbs Excess Adsorption Thermodynamics and Poromechanics of Nanoporous Materials*, Sixth Biot Conference on Poromechanics, 2017; pp 56−63.
(26) Dubinin, M. M. Physical Adsorption of Gases and Vapors in Micropores. In *Progress in Surface and Membrane Science*; Elsevier, 1975; Vol. *9*, pp 1−70.
(27) Dubinin, M. M.; Stoeckli, H. F. Homogeneous and heterogeneous micropore structures in carbonaceous adsorbents. *J. Colloid Interface Sci.* **1980**, *75*, 34−42.
(28) Shkolin, A. V.; Fomkin, A. A.; Sinitsyn, V. A. Adsorption-Induced Deformation of AUK Microporous Carbon Adsorbent in Adsorption of n-Pentane. *Prot. Met. Phys. Chem. Surf.* **2011**, *47*, 555−561.
(29) Hückel, E. *Adsorption und Kapillarkondensation*; Akademische Verlagsgesellschaft M.B.H.: Leipzig, 1928; p 320.
(30) Mogilnikov, K. P.; Baklanov, M. R. Determination of Young's modulus of porous low-k films by ellipsometric porosimetry. *Electrochem. Solid-State Lett.* **2002**, *5*, F29−F31.
(31) Prass, J.; Müter, D.; Fratzl, P.; Paris, O. Capillarity-driven deformation of ordered nanoporous silica. *Appl. Phys. Lett.* **2009**, *95*, No. 083121.
(32) Balzer, C.; Waag, A. M.; Gehret, S.; Reichenauer, G.; Putz, F.; Hüsing, N.; Paris, O.; Bernstein, N.; Gor, G. Y.; Neimark, A. V. Adsorption-Induced Deformation of Hierarchically Structured Mesoporous Silica Effect of Pore-Level Anisotropy. *Langmuir* **2017**, *33*, 5592−5602.
(33) Nabiulin, V. V.; Fomkin, A. A.; Tvardovskii, A. V. Adsorption deformation of a microporous AR-V carbon adsorbent during the adsorption of benzene. *Prot. Met. Phys. Chem. Surf.* **2012**, *48*, 398−401.
(34) Nabiulin, V. V.; Fomkin, A. A.; Tvardovskiy, A. V. Adsorption deformation of a microporous AR-V carbon adsorbent during the adsorption of n-hexane. *Russ. J. Phys. Chem. A* **2011**, *85*, 1960−1964.
(35) Odell Wood, G. Activated carbon adsorption capacities for vapors. *Carbon* **1992**, *30*, 593−599.
(36) Férey, G.; Serre, C. Large breathing effects in three-dimensional porous hybrid matter: facts, analyses, rules and consequences. *Chem. Soc. Rev.* **2009**, *38*, 1380.
(37) Cheng, Y.; Kajiro, H.; Noguchi, H.; Kondo, A.; Ohba, T.; Hattori, Y.; Kaneko, K.; Kanoh, H. Tuning of Gate Opening of an Elastic Layered Structure MOF in CO2 Sorption with a Trace of Alcohol Molecules. *Langmuir* **2011**, *27*, 6905−6909.
(38) Coudert, F.-X.; Boutin, A.; Fuchs, A. H.; Neimark, A. V. Adsorption Deformation and Structural Transitions in Metal−Organic Frameworks: From the Unit Cell to the Crystal. *J. Phys. Chem. Lett.* **2013**, *4*, 3198−3205.
(39) Neimark, A. V.; Coudert, F.-X.; Boutin, A.; Fuchs, A. H. Stress-Based Model for the Breathing of Metal-Organic Frameworks. *J. Phys. Chem. Lett.* **2010**, *1*, 445−449.

DOI: 10.1021/acs.jpcc.9b10053
J. Phys. Chem. C 2020, 124, 749−755